Unified Probabilistic Approach for Model Updating and Damage Detection

Ka-Veng Yuen
Department of Civil and Environmental Engineering,
University of Macau,
Macau, China
e-mail: kvyuen@umac.mo

James L. Beck
Division of Engineering and Applied Science,
California Institute of Technology,
Mail Code 104-44,
Pasadena, CA 91125
e-mail: jimbeck@caltech.edu

Lambros S. Katafygiotis
Department of Civil Engineering,
Hong Kong University of Science and Technology,
Clearwater Bay,
Kowloon, Hong Kong

A probabilistic approach for model updating and damage detection of structural systems is presented using noisy incomplete input and incomplete response measurements. The situation of incomplete input measurements may be encountered, for example, during low-level ambient vibrations when a structure is instrumented with accelerometers that measure the input ground motion and the structural response at a few instrumented locations but where other excitations, e.g., due to wind, are not measured. The method is an extension of a Bayesian system identification approach developed by the authors. A substructuring approach is used for the parameterization of the mass, damping and stiffness distributions. Damage in a substructure is defined as stiffness reduction established through the observation of a reduction in the values of the various substructure stiffness parameters compared with their initial values corresponding to the undamaged structure. By using the proposed probabilistic methodology, the probability of various damage levels in each substructure can be calculated based on the available dynamic data. Examples using a single-degree-of-freedom oscillator and a 15-story building are considered to demonstrate the proposed approach. [DOI: 10.1115/1.2150235]

1 Introduction

The problem of identification of the model parameters of a linear structural model using dynamic data has received much attention over the years because of its importance in model updating, response prediction, structural control and health monitoring. Many methodologies have been formulated, both in the time and frequency domain, for the cases of known and unknown input.

Structural health monitoring has been attracting much attention in the past two decades, including several workshops, e.g., Natke and Yao [1]; Agbabian and Masri [2]; Chang [3]; and special issues of journals, e.g., Journal of Engineering Mechanics (July 2000 and January 2004) and Computer-Aided Civil and Infrastructure Engineering (January 2001). Many methods have been developed. One such example is the class of direct methods using pattern recognition techniques (Mazurek and DeWolf [4]; Hearn and Testa [5]; Doebling et al. [6]; Lam et al. [7]; Smyth et al. [8]). Another example is the class of structural model-based inverse methods (Farhat and Hemez [9]; Pandey and Biswas [10]; Kim et al. [11]; Topole and Stubbs [12]; Hemez and Farhat [13]; Katafygiotis et al. [14]; Doebling et al. [15]; Vanik et al. [16]; Beck et al. [17]; Sohn and Farrar [18]; Ko et al. [19]; Ching and Beck [20]).

Recent interest has been shown in using Bayesian probabilistic approaches for model updating and damage detection as they allow for an explicit treatment of all the uncertainties involved (Geyskens et al. [21]; Beck and Katafygiotis [22]; Katafygiotis et al. [14]; Vanik et al. [16]; Katafygiotis and Yuen [23]; Yuen [24]). An advantage of the Bayesian approach is that it follows directly from the probability axioms and so there are no ad-hoc assumptions that lead to loss of information. In Beck and Katafygiotis [22], a methodology for model updating based on a Bayesian probabilistic system identification framework was presented. Although the framework is general, their presentation is for the case where the prediction error due to measurement noise and modeling error is modeled as Gaussian white noise.

In the present paper, the prediction error is modeled as the sum of a filtered white noise process, representing the input error (measurement noise plus unmeasured excitation) filtered through the system, plus another independent white noise process, representing the response measurement noise and modeling error. A Bayesian time-domain approach for modal identification by Yuen and Katafygiotis [25] is extended to handle the case of model updating with incomplete input measurements and with measurement noises in both input and output measurements. The proposed approach allows for the direct calculation of the probability density function (PDF) of the model parameters based on the data which can be then approximated by an appropriately selected multi-variate Gaussian distribution. By using data from the initial undamaged state and a later possibly damaged state, the probability of damage of various levels in specified substructures may be calculated. The formulation is presented for linear multi-degree-of-freedom (MDOF) systems. Examples using noisy simulated data from a single-degree-of-freedom (SDOF) oscillator and a 15-story building are given for illustration.

2 Model Formulation

2.1 Class of Structural Models. Consider a class of possible models for a structural system with N_d degrees of freedom (DOFs) and equation of motion

$$\mathbf{M}\ddot{\mathbf{x}} + \mathbf{C}\dot{\mathbf{x}} + \mathbf{K}\mathbf{x} = \mathbf{T}\mathbf{g} \tag{1}$$

where $\mathbf{M}$, $\mathbf{C}$, and $\mathbf{K}$ are the mass, damping and stiffness matrix of the system, respectively, $\mathbf{g} \in \mathbb{R}^{N_g}$ is the actual forcing vector and $\mathbf{T} \in \mathbb{R}^{N_d \times N_g}$ is the forcing distribution matrix. The mass, damping and stiffness matrices, $\mathbf{M}$, $\mathbf{C}$, and $\mathbf{K}$, are defined in terms of mass, damping and stiffness parameters $\boldsymbol{\theta}_m$, $\boldsymbol{\theta}_c$, and $\boldsymbol{\theta}_s$ by

$$\mathbf{M} = \sum_{j=1}^{N_{\text{sub}}} \mathbf{M}_j(\boldsymbol{\theta}_m), \quad \mathbf{C} = \sum_{j=1}^{N_{\text{sub}}} \mathbf{C}_j(\boldsymbol{\theta}_c), \quad \mathbf{K} = \sum_{j=1}^{N_{\text{sub}}} \mathbf{K}_j(\boldsymbol{\theta}_s) \tag{2}$$

where N_{sub} is the number of substructures and $\mathbf{M}_j$, $\mathbf{C}_j$, and $\mathbf{K}_j$ are the contributions to the mass, damping and stiffness matrix of the

Contributed by the Applied Mechanics Division of ASME for publication in the JOURNAL OF APPLIED MECHANICS. Manuscript received July 11, 2004; final manuscript received September 29, 2005. Review conducted by I. Mezic. Discussion on the paper should be addressed to the Editor, Prof. Robert M. McMeeking, Journal of Applied Mechanics, Department of Mechanical and Environmental Engineering, University of California—Santa Barbara, Santa Barbara, CA 93106-5070, and will be accepted until four months after final publication in the paper itself in the ASME JOURNAL OF APPLIED MECHANICS.

jth substructure, respectively. Note that it is not necessary to require classical normal modes.

2.2 Stochastic Input Model. Assume that discrete-time input data $\{\mathbf{f}[k]:k=1,\ldots,N\}$ are available for the excitation where the index k refers to time $(k-1)\Delta t$ with Δt being the sampling interval. Define the uncertain input error $\boldsymbol{\eta}_f$ by

$$\mathbf{g}[k]=\mathbf{f}[k]+\boldsymbol{\eta}_f[k] \tag{3}$$

The input error $\boldsymbol{\eta}_f$ is modeled as zero-mean Gaussian discrete white noise with covariance matrix $\Sigma_{\eta f}(\boldsymbol{\theta}_\eta)$, where $\boldsymbol{\theta}_\eta$ is the parameter vector defining the covariance matrices of the input and output errors; this PDF maximizes the information entropy of the input error for a specified mean and covariance matrix. The components of $\mathbf{f}[k]$ that correspond to the unobserved excitation components of $\mathbf{g}[k]$ are set equal to zero. Thus, $\boldsymbol{\eta}_f$ models the input measurement noise for the observed components and it models the unobserved excitation for the unobserved components. The advantage of this formulation is that it can handle cases that include complete excitation measurements, incomplete excitation measurements and no excitation measurements (such as in ambient vibration tests).

2.3 Stochastic Output Model. Assume that discrete-time response data are available at N_o observed DOFs where the measured response $\mathbf{z}[k]\in\mathbb{R}^{N_o}$ is a linear combination of the model state vector $\mathbf{y}[k]=[\mathbf{x}[k]^T,\dot{\mathbf{x}}[k]^T]^T$ and the actual force $\mathbf{g}[k]$, plus an output error $\boldsymbol{\eta}_z[k]\in\mathbb{R}^{N_o}$ that accounts for modeling error and measurement noise in the response measurements. This output error is modeled as zero-mean Gaussian discrete white noise with covariance matrix $\Sigma_{\eta z}(\boldsymbol{\theta}_\eta)$. Thus, the measured response is given by

$$\mathbf{z}[k]=\mathbf{L}_1\mathbf{y}[k]+\mathbf{L}_2\mathbf{g}[k]+\boldsymbol{\eta}_z[k]=\mathbf{L}_1\mathbf{y}[k]+\mathbf{L}_2\mathbf{f}[k]+\mathbf{L}_2\boldsymbol{\eta}_f[k]+\boldsymbol{\eta}_z[k] \tag{4}$$

where $\mathbf{L}_1\in\mathbb{R}^{N_o\times 2N_d}$ and $\mathbf{L}_2\in\mathbb{R}^{N_o\times N_g}$ are observation matrices that depend on the type of measurements (e.g., displacements or accelerations), and $\mathbf{y}[k]$ is given by Eq. (1). Furthermore, the errors $\boldsymbol{\eta}_z$ and $\boldsymbol{\eta}_f$ are modeled as stochastically independent.

2.4 Model and Damage Identification. The parameter vector $\boldsymbol{\theta}$ for identification from the excitation and response data is comprised of: (1) the mass, damping, and stiffness parameters $\boldsymbol{\theta}_m$, $\boldsymbol{\theta}_c$, and $\boldsymbol{\theta}_s$ that specify the mass matrix $\mathbf{M}$, damping matrix $\mathbf{C}$, and stiffness matrix $\mathbf{K}$; (2) the parameter vector $\boldsymbol{\theta}_\eta$ specifying the covariance matrices for the input and output errors $\boldsymbol{\eta}_f$ and $\boldsymbol{\eta}_z$, respectively; and (3) the $2N_d$ initial conditions for the structural state. In practice, the system may often be assumed to start from rest. In such a case, the initial conditions can be treated as known and equal to zero and can be excluded from the vector $\boldsymbol{\theta}$ of parameters for identification.

Let $\mathbf{Z}_{m,n}$ and $\mathbf{F}_{m,n}$ denote the response and the excitation measurement matrix from time $(m-1)\Delta t$ to $(n-1)\Delta t$, with $m\leq n$, respectively,

$$\mathbf{Z}_{m,n}=[\mathbf{z}[m],\ldots,\mathbf{z}[n]] \quad \text{and} \quad \mathbf{F}_{m,n}=[\mathbf{f}[m],\ldots,\mathbf{f}[n]], \quad m\leq n \tag{5}$$

The approach to damage detection is to first use the Bayesian framework presented in the next section to obtain the updated PDF (probability density function) $p(\boldsymbol{\theta}|\mathbf{Z}_{1,N},\mathbf{F}_{1,N})$ of the parameter vector $\boldsymbol{\theta}$ given the measured input data $\mathbf{F}_{1,N}$ and output data $\mathbf{Z}_{1,N}$ where N denotes the total number of points in time where measurements are available. Then, this is used to compute the probability of damage of the jth substructure exceeding damage level d which is defined by

$$P_j^{\text{dam}}(d)\equiv P\{\theta_j^{\text{pd}}<(1-d)\,\theta_j^{\text{ud}}|\mathbf{F}_{1,N}^{\text{ud}},\mathbf{Z}_{1,N}^{\text{ud}},\mathbf{F}_{1,N}^{\text{pd}},\mathbf{Z}_{1,N}^{\text{pd}}\} \tag{6}$$

where subscripts "ud" and "pd" refer to undamaged and possibly damaged cases. Equation (6) gives the probability that the substructure stiffness parameter has decreased by a fractional amount of more than d. Based on the Gaussian approximation of the updated PDFs for θ_j^{ud} and θ_j^{pd}, one can easily calculate the probability damage as follows (Yuen et al. [26])

$$P_j^{\text{dam}}(d)\approx\Phi\left(\frac{(1-d)\,\hat{\theta}_j^{\text{ud}}-\hat{\theta}_j^{\text{pd}}}{\sqrt{(1-d)^2(\hat{\sigma}_j^{\text{ud}})^2+(\hat{\sigma}_j^{\text{pd}})^2}}\right) \tag{7}$$

where $\Phi(\cdot)$ is the standard Gaussian cumulative distribution function; $\hat{\theta}_j^{\text{ud}}$ and $\hat{\theta}_j^{\text{pd}}$ denote the most probable values of the stiffness parameters for the undamaged and (possibly) damaged structure, respectively; and $\hat{\sigma}_j^{\text{ud}}$ and $\hat{\sigma}_j^{\text{pd}}$ are the corresponding standard deviations of the stiffness parameters determined from the inverse of the Hessian matrix of the negative logarithm of the joint updated parameter PDF (Beck and Katafygiotis [22]).

3 Bayesian Model Updating

3.1 Exact Formulation of Updating. Using Bayes' theorem, the expression for the updated (posterior) PDF of the parameters $\boldsymbol{\theta}$ given the measured response $\mathbf{Z}_{1,N}$ and the measured input $\mathbf{F}_{1,N}$ is

$$p(\boldsymbol{\theta}|\mathbf{Z}_{1,N},\mathbf{F}_{1,N})=c_1p(\boldsymbol{\theta})p(\mathbf{Z}_{1,N}|\boldsymbol{\theta},\mathbf{F}_{1,N}) \tag{8}$$

where c_1 is a normalizing constant such that the integral of the right hand side of Eq. (8) over the domain of $\boldsymbol{\theta}$ is equal to unity. We interpret $p(\boldsymbol{\theta}|\mathbf{Z}_{1,N},\mathbf{F}_{1,N})$ as giving a measure of the plausibility of the values of $\boldsymbol{\theta}$ based on the data (Jaynes [27]). The factor $p(\boldsymbol{\theta})$ in Eq. (8) denotes the prior PDF of the parameters and it may be chosen based on engineering judgment. It may be treated as constant (noninformative prior) if all values of the parameters over some large but finite domain are felt to be equally plausible a priori. The likelihood $p(\mathbf{Z}_{1,N}|\boldsymbol{\theta},\mathbf{F}_{1,N})$ is the dominant factor on the right hand side of Eq. (8). It reflects the contribution of the measured data $\mathbf{Z}_{1,N}$ and $\mathbf{F}_{1,N}$ in establishing the updated PDF of $\boldsymbol{\theta}$. Also, in order to establish the most probable (plausible) value of $\boldsymbol{\theta}$, denoted by $\hat{\boldsymbol{\theta}}$, one therefore needs to maximize $p(\boldsymbol{\theta})p(\mathbf{Z}_{1,N}|\boldsymbol{\theta},\mathbf{F}_{1,N})$.

Since linear systems are considered and both the uncertain input and output measurement noise and unmeasured excitation are modeled as Gaussian, it follows that the likelihood $p(\mathbf{Z}_{1,N}|\boldsymbol{\theta},\mathbf{F}_{1,N})$ in Eq. (8) is an N_oN-variate Gaussian distribution with appropriately calculated mean and covariance matrix. Direct calculation of this function for different values of $\boldsymbol{\theta}$ becomes computationally prohibitive for a large number N of data, as it requires repeated calculation of the determinant and inverse of the corresponding very high-dimensional $N_oN\times N_oN$ covariance matrices. Thus, although Eq. (8) offers a theoretically exact solution to the model updating problem, its computational implementation poses a challenge. In the next section, an approximation is presented which overcomes this difficulty and renders the Bayesian model updating problem computationally feasible.

3.2 Proposed Approximation for the Likelihood. The PDF $p(\mathbf{Z}_{1,N}|\boldsymbol{\theta},\mathbf{F}_{1,N})$ in Eq. (8) can be written as a product of conditional PDFs

$$p(\mathbf{Z}_{1,N}|\boldsymbol{\theta},\mathbf{F}_{1,N})=p(\mathbf{Z}_{1,N_p}|\boldsymbol{\theta},\mathbf{F}_{1,N})\prod_{k=N_p+1}^{N}p(\mathbf{z}[k]|\boldsymbol{\theta},\mathbf{Z}_{1,k-1},\mathbf{F}_{1,N}) \tag{9}$$

The following approximation is introduced [25]

$$p(\mathbf{Z}_{1,N}|\boldsymbol{\theta},\mathbf{F}_{1,N}) \approx p(\mathbf{Z}_{1,N_p}|\boldsymbol{\theta},\mathbf{F}_{1,N}) \prod_{k=N_p+1}^{N} p(\mathbf{z}[k]|\boldsymbol{\theta},\mathbf{Z}_{k-N_p,k-1},\mathbf{F}_{1,N}) \quad (10)$$

Here, each conditional PDF factor depending on all the previous response measurements is approximated by a conditional PDF depending on only the most recent N_p response measurements. The sense of this approximation is that response measurements too far in the past do not provide significant information about the present observed response. Of course, one expects this to be true if N_p is so large that all the correlation functions have decayed to very small values. However, it is found that a significantly smaller value of N_p suffices for the approximation in Eq. (10) to be valid for practical purposes. In particular, it is found that a value for N_p of the order of $T_1/\Delta t$ is sufficient, where T_1 is the fundamental period of the system and Δt is the sampling interval. For example, assuming $\Delta t = \frac{1}{25}T_1$, it follows that a value of $N_p=25$ is sufficient. The advantage of the approximation in Eq. (10) will become obvious in the subsequent sections where the expressions for computing the factors on the right hand side of Eq. (10) are given. In Sec. 3.2.1, the expression for the first factor $p(\mathbf{Z}_{1,N_p}|\boldsymbol{\theta},\mathbf{F}_{1,N})$ in Eq. (10) is given. In Sec. 3.2.2, a general expression for the conditional PDF $p(\mathbf{z}[k]|\boldsymbol{\theta},\mathbf{Z}_{k-N_p,k-1},\mathbf{F}_{1,N})$ in Eq. (10) is derived. Based on these results, $p(\mathbf{Z}_{1,N}|\boldsymbol{\theta},\mathbf{F}_{1,N})$ can be computed efficiently from Eq. (10).

The most probable parameters $\hat{\boldsymbol{\theta}}$ can then be obtained by minimizing $J(\boldsymbol{\theta})=-\ln[p(\boldsymbol{\theta})p(\mathbf{Z}_{1,N}|\boldsymbol{\theta},\mathbf{F}_{1,N})]$. Also, the updated PDF of the parameters $\boldsymbol{\theta}$ can be well approximated by a Gaussian distribution $\mathcal{N}(\hat{\boldsymbol{\theta}},\mathbf{H}(\hat{\boldsymbol{\theta}})^{-1})$ with mean $\boldsymbol{\theta}$ and covariance matrix $\mathbf{H}(\hat{\boldsymbol{\theta}})^{-1}$, where $\mathbf{H}(\hat{\boldsymbol{\theta}})$ denotes the Hessian of $J(\boldsymbol{\theta})$ calculated at $\boldsymbol{\theta}=\hat{\boldsymbol{\theta}}$ (Beck and Katafygiotis [22]).

3.2.1 Expression for $p(\mathbf{Z}_{1,N_p}|\boldsymbol{\theta},\mathbf{F}_{1,N})$. Since the joint PDF $p(\mathbf{Z}_{1,N_p}|\boldsymbol{\theta},\mathbf{F}_{1,N})$ follows an N_oN_p-variate Gaussian distribution, it is specified by the mean and covariance matrix of $\mathbf{Z}_{1,N}$. Expressions for the mean and covariance are derived as a function of the identification parameter vector $\boldsymbol{\theta}$ as follows.

The equation of motion (1) can be rewritten in a state space form for the structural state vector $\mathbf{y}\equiv[\mathbf{x}^T,\dot{\mathbf{x}}^T]^T$

$$\dot{\mathbf{y}} = \mathbf{A}\mathbf{y} + \mathbf{B}\mathbf{g} \quad (11)$$

where the system matrices $\mathbf{A}\in\mathbb{R}^{2N_d\times 2N_d}$ and $\mathbf{B}\in\mathbb{R}^{2N_d\times N_g}$ are given by

$$\mathbf{A} = \begin{bmatrix} \mathbf{0}_{N_d} & \mathbf{I}_{N_d} \\ -\mathbf{M}^{-1}\mathbf{K} & -\mathbf{M}^{-1}\mathbf{C} \end{bmatrix} \quad (12)$$

and $\mathbf{B}=\left[\begin{smallmatrix} 0_{N_d} \\ \mathbf{M}^{-1}\end{smallmatrix}\right]\mathbf{T}$. Here, 0_{N_d} and $\mathbf{I}_{N_d}$ denote the $N_d\times N_d$ zero and identity matrix, respectively.

The continuous-time differential Eq. (11) is approximated by the following difference equation

$$\mathbf{y}[k+1] = \mathbf{A}_d\mathbf{y}[k] + \mathbf{B}_d\mathbf{g}[k] \quad (13)$$

where $\mathbf{y}[k]$ denotes the structural state vector at time $t_k=(k-1)\Delta t$, $\mathbf{A}_d\equiv e^{\mathbf{A}\Delta t}$ and $\mathbf{B}_d\equiv\mathbf{A}^{-1}(\mathbf{A}_d-\mathbf{I}_{2N_d})\mathbf{B}$. For notation convenience, denote the relationship between the state vector and the input of the above system using the function $\mathcal{L}$

$$\mathbf{y}[k] \equiv \mathcal{L}(k;\boldsymbol{\theta},\mathbf{G}_{1,N}), \quad k\leqslant N \quad (14)$$

where $\boldsymbol{\theta}$ is the vector comprised of the model parameters for identification described earlier and $\mathbf{G}_{1,N}$ denotes, in analogy to the definition of Eq. (5), the matrix comprised of the actual input force time history up to time $(N-1)\Delta t$, i.e., $\mathbf{G}_{1,N}=[\mathbf{g}[1],\mathbf{g}[2],\ldots,\mathbf{g}[N]]$.

It can be easily shown using Eq. (4) that the mean $\boldsymbol{\mu}[k]\equiv E[\mathbf{z}[k]|\boldsymbol{\theta},\mathbf{F}_{1,N}]$ is given by

$$\boldsymbol{\mu}[k] = \mathbf{L}_1\mathcal{L}(k;\boldsymbol{\theta},\mathbf{F}_{1,N}) + \mathbf{L}_2\mathbf{f}[k] \quad (15)$$

Thus, $\boldsymbol{\mu}[k]$ is equal to the model response calculated assuming that the only input is the measured excitation. The difference between $\mathbf{z}[k]$ and $\boldsymbol{\mu}[k]$ is the prediction error $\boldsymbol{v}[k]$

$$\boldsymbol{v}[k] = \mathbf{z}[k] - \boldsymbol{\mu}[k] \quad (16)$$

It is worth noting that $\boldsymbol{\mu}[k]$ in Eq. (15) can be simply calculated using the function "lsim" in MATLAB [28]. Collecting all the terms calculated by Eq. (15), $E(\mathbf{Z}_{1,N_p}|\boldsymbol{\theta},\mathbf{F}_{1,N})$ is given by

$$E(\mathbf{Z}_{1,N_p}|\boldsymbol{\theta},\mathbf{F}_{1,N}) = [\boldsymbol{\mu}[1]^T,\ldots,\boldsymbol{\mu}[N_p]^T]^T \quad (17)$$

The covariance matrix $\Sigma_{Z,N_p}\equiv E[[\mathbf{Z}_{1,N_p}-E(\mathbf{Z}_{1,N_p}|\boldsymbol{\theta},\mathbf{F}_{1,N})]\times[\mathbf{Z}_{1,N_p}-E(\mathbf{Z}_{1,N_p}|\boldsymbol{\theta},\mathbf{F}_{1,N})]^T]$ is given by

$$\Sigma_{Z,N_p} = \begin{bmatrix} \Sigma_v[1,1] & \cdots & \Sigma_v[1,N_p] \\ & \ddots & \vdots \\ \text{sym} & & \Sigma_v[N_p,N_p] \end{bmatrix} \quad (18)$$

where $\Sigma_v[m,n]$, $m\leqslant n$, can be approximated by (see Appendix A)

$$\Sigma_v[m,n] \approx \mathbf{L}_1\mathbf{S}_\infty(\mathbf{A}_d^T)^{n-m}\mathbf{L}_1^T + \mathbf{L}_2\Sigma_{\eta f}\mathbf{B}_d^T(\mathbf{A}_d^T)^{n-m-1}\mathbf{L}_1^T(1-\delta_{m,n}) + (\mathbf{L}_2\Sigma_{\eta f}\mathbf{L}_2^T + \Sigma_{\eta z})\delta_{m,n} \quad (19)$$

where $\delta_{m,n}$ is the Kronecker delta and the matrix $\mathbf{S}_\infty$ can be obtained by solving the Lyapunov equation in discrete form (Lin [29])

$$\mathbf{S}_\infty = \mathbf{A}_d\mathbf{S}_\infty\mathbf{A}_d^T + \mathbf{B}_d\Sigma_{\eta f}\mathbf{B}_d^T \quad (20)$$

Furthermore, $\Sigma_v[n,m]=\Sigma_v[m,n]^T$, $m\leqslant n$, defines the elements in the lower triangle.

The joint PDF $p(\mathbf{Z}_{1,N_p}|\boldsymbol{\theta},\mathbf{F}_{1,N})$ is then the N_oN_p-variate Gaussian distribution

$$p(\mathbf{Z}_{1,N_p}|\boldsymbol{\theta},\mathbf{F}_{1,N}) = \frac{1}{(2\pi)^{N_oN_p/2}|\Sigma_{Z,N_p}|^{1/2}} \times\exp\left\{-\frac{1}{2}[\mathbf{Z}_{1,N_p}-E(\mathbf{Z}_{1,N_p}|\boldsymbol{\theta},\mathbf{F}_{1,N})]^T \times\Sigma_{Z,N_p}^{-1}[\mathbf{Z}_{1,N_p}-E(\mathbf{Z}_{1,N_p}|\boldsymbol{\theta},\mathbf{F}_{1,N})]\right\} \quad (21)$$

3.2.2 Expression for $p(\mathbf{z}[k]|\boldsymbol{\theta},\mathbf{Z}_{k-N_p,k-1},\mathbf{F}_{1,N})$. Define the vector $\mathbf{W}[k]$, $k>N_p$, as follows: $\mathbf{W}[k]=[\mathbf{z}[k]^T,\mathbf{z}[k-1]^T,\ldots,\mathbf{z}[k-N_p]^T]^T$, which is comprised of all the response measurements appearing in $p(\mathbf{z}[k]|\boldsymbol{\theta},\mathbf{Z}_{k-N_p,k-1},\mathbf{F}_{1,N})$. Specifically, $\mathbf{W}[k]$ consists of $\mathbf{z}[k]$ followed by all vector elements of $\mathbf{Z}_{k-N_p,k-1}$ ordered in a descending time index order. Next, the expressions for the mean value and the covariance of the Gaussian joint PDF $p(\mathbf{W}[k]|\boldsymbol{\theta},\mathbf{F}_{1,N})$ are derived.

Clearly, the expected value of the vector $\mathbf{W}[k]$ given $\boldsymbol{\theta}$ and $\mathbf{F}_{1,N}$ is given by

$$E[\mathbf{W}[k]|\boldsymbol{\theta},\mathbf{F}_{1,N}] = [\boldsymbol{\mu}[k]^T,\boldsymbol{\mu}[k-1]^T,\ldots,\boldsymbol{\mu}[k-N_p]^T]^T \quad (22)$$

where $\boldsymbol{\mu}[k]$ is given by Eq. (15). The covariance matrix $\Sigma_W[k]=E\{[\mathbf{W}[k]-E(\mathbf{W}[k]|\boldsymbol{\theta},\mathbf{F}_{1,N})][\mathbf{W}[k]-E(\mathbf{W}[k]|\boldsymbol{\theta},\mathbf{F}_{1,N})]^T\}$ given $\mathbf{F}_{1,N}$ is easily shown to be

$$\Sigma_W[k] = \begin{bmatrix} \Sigma_v[k,k] & & \text{sym} \\ \vdots & \ddots & \\ \Sigma_v[k-N_p,k] & \cdots & \Sigma_v[k-N_p,k-N_p] \end{bmatrix} \quad (23)$$

where $\Sigma_v[m,n]$, $m\leqslant n$ is given by Eq. (19) and $\Sigma_v[n,m]=\Sigma_v[m,n]^T$, $m\leqslant n$. Therefore, the joint PDF $p(\mathbf{W}[k]|\boldsymbol{\theta},\mathbf{F}_{1,N})$, $N_p+1\leqslant k\leqslant N$, is an $N_o(N_p+1)$-variate Gaussian distribution with mean given by Eq. (22) and covariance matrix $\Sigma_W[k]$ given by Eq. (23) which is independent of k when the approximation for

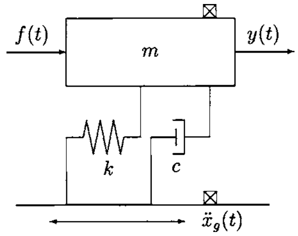

Fig. 1 Single-degree-of-freedom oscillator model (Example 1)

Table 1 Identification results of the stiffness parameters of the oscillator (Example 1)

Parameter	Actual $\tilde{\theta}$	Optimal $\hat{\theta}$	S.D. σ	COV α	β
k	100.00	100.32	1.3490	0.014	0.23
c	0.4000	0.5423	0.1391	0.348	1.02
$\sigma_{\eta f}$	2.5005	2.4476	0.0939	0.038	0.56
$\sigma_{\eta z}$	0.0036	0.0035	0.0001	0.016	1.24

$\Sigma_v[m,n]$ in Eq. (19) is used. Then, the matrix Σ_W is partitioned as follows:

$$\Sigma_W = \begin{bmatrix} \Sigma_{11} & \Sigma_{12} \\ \Sigma_{12}^T & \Sigma_{22} \end{bmatrix} \tag{24}$$

where Σ_{11}, Σ_{12}, and Σ_{22} have dimensions $N_o \times N_o$, $N_o \times N_o N_p$, and $N_o N_p \times N_o N_p$, respectively.

The mean and covariance matrix for the N_o-variate Gaussian PDF $p(\mathbf{z}[k]|\boldsymbol{\theta},\mathbf{Z}_{k-N_p,k-1},\mathbf{F}_{1,N})$ can be determined from the corresponding mean and covariance matrix for $\mathbf{W}[k]$ given $\boldsymbol{\theta}$ and $\mathbf{F}_{1,N}$. The mean $\mathbf{e}[k] \equiv E[\mathbf{z}[k]|\boldsymbol{\theta},\mathbf{Z}_{k-N_p,k-1},\mathbf{F}_{1,N}]$ is given by

$$\mathbf{e}[k] = \boldsymbol{\mu}[k] + \Sigma_{12}\Sigma_{22}^{-1}[\boldsymbol{v}[k-1]^T, \boldsymbol{v}[k-2]^T, \ldots, \boldsymbol{v}[k-N_p]^T]^T \tag{25}$$

where $\boldsymbol{\mu}[k]$ is given by Eq. (15) and the prediction errors $\boldsymbol{v}[m]$, $m=k-N_p,\ldots,k-1$, are given by Eq. (16). The covariance matrix $\Sigma_{\epsilon,N_p}[k]$ of the error $\boldsymbol{\epsilon}[k]=\mathbf{z}[k]-\mathbf{e}[k]$ is given by

$$\Sigma_{\epsilon,N_p}[k] \equiv E[\boldsymbol{\epsilon}[k]\boldsymbol{\epsilon}[k]^T] = \Sigma_{11} - \Sigma_{12}\Sigma_{22}^{-1}\Sigma_{12}^T \tag{26}$$

which does not depend on k when the approximation for $\Sigma_v[m,n]$ in Eq. (19) is used. Thus, the conditional PDF $p(\mathbf{z}[k]|\boldsymbol{\theta},\mathbf{Z}_{k-N_p,k-1},\mathbf{F}_{1,N})$ is given by the following Gaussian distribution

$$p(\mathbf{z}[k]|\boldsymbol{\theta},\mathbf{Z}_{k-N_p,k-1},\mathbf{F}_{1,N}) \approx \frac{1}{(2\pi)^{N_o/2}|\Sigma_{\epsilon,N_p}|^{1/2}} \exp\left\{-\frac{1}{2}(\mathbf{z}[k] - \mathbf{e}[k])^T \Sigma_{\epsilon,N_p}^{-1}(\mathbf{z}[k]-\mathbf{e}[k])\right\} \tag{27}$$

where $\mathbf{e}[k]$ is given by Eq. (25) and Σ_{ϵ,N_p} is given by Eq. (26). It is of interest to note that this probability distribution is equivalent to taking an auto-regressive model of order N_p for the prediction error $v[k]$ in Eq. (16).

The advantage of the approximation introduced in Eq. (10) is that all the conditional PDFs on the right hand side of Eq. (10) are conditioned on exactly N_p previous response measurement points and follow an N_o-variate Gaussian distribution with approximately the same covariance matrix Σ_{ϵ,N_p} which, therefore, needs to be calculated only once for a given parameter set $\boldsymbol{\theta}$. Thus, to compute $p(\mathbf{Z}_{1,N}|\boldsymbol{\theta},\mathbf{F}_{1,N})$, one needs to calculate the inverse and the determinant of only the matrices Σ_{Z,N_p}, Σ_{22}, and Σ_{ϵ,N_p}, of dimension $N_oN_p \times N_oN_p$, $N_oN_p \times N_oN_p$, and $N_o \times N_o$, respectively. This effort is much smaller than that required in an exact formulation where one needs to calculate the inverse and the determinant of a matrix of dimension $N_oN \times N_oN$, where $N \gg N_p$ in general.

4 Illustrative Examples

4.1 Example 1: SDOF Oscillator. Consider a SDOF oscillator of mass $m=1$ kg subjected to external force $f(t)$ and base acceleration $\ddot{x}_g(t)$, as shown in Fig. 1. Here, $f(t)$ is white noise with spectral intensity $S_{f0}=0.02$ N^2 s and the base acceleration is taken to be the 1940 El-Centro earthquake record in the N-S direction. The parameters $\tilde{\boldsymbol{\theta}}=[\tilde{k},\tilde{c},\tilde{\sigma}_{\eta f},\tilde{\sigma}_{\eta z}]^T$ used to generate the simulated data are: $\tilde{k}=100.0$ N/m, $\tilde{c}=0.04$ N s/m (corresponding to damping ratio of 2.0%), $\tilde{S}_{f0}=0.02$ N^2 s, $\tilde{\sigma}_{\eta f}=2.5005$ N and $\tilde{\sigma}_{\eta z}=0.0036$ m. The chosen value of $\tilde{\sigma}_{\eta f}$ corresponds to the standard deviation combining the unmeasured input f and 10% measurement noise of the measured input $\ddot{x}_g$. Also, the chosen value of $\tilde{\sigma}_{\eta z}$ corresponds to a 10% rms output-error level, i.e., the noise is 10% of the rms of the noise-free response. The sampling time step is taken to be 0.02 s and the total time interval is $T=50$ s, about 80 fundamental periods, so that the number of data points is $N=2500$.

Table 1 refers to the identification results using a single set of displacement response measurements $\hat{\mathbf{Z}}_{1,N}$ and base acceleration measurements $\hat{\mathbf{F}}_{1,N}$. It shows the exact values of the parameters, the most probable values $\hat{\boldsymbol{\theta}}=[\hat{k},\hat{c},\hat{\sigma}_{\eta f},\hat{\sigma}_{\eta z}]^T$, the calculated standard deviations for the Gaussian approximation of the joint PDF of k, c, $\sigma_{\eta f}$, and $\sigma_{\eta z}$, the coefficient of variation for each parameter and the value of a "normalized error" β for each parameter. The parameter β represents the absolute value of the difference between the identified value and exact value, normalized with respect to the corresponding calculated standard deviation. Here, the value $N_p=30$ (corresponding to one period of the oscillator) was used in Eq. (10). Note that the order of the square matrices that need to be inverted by the proposed approach is $N_p=30$ which is much smaller than $N=2500$ in an exact formulation. Repeating the identification with a value of $N_p=60$ yielded identical results to the accuracy shown, verifying that using $N_p=T_1/\Delta t$ is sufficient.

Figure 2 shows contours in the (k,c) plane of the marginal updated PDF $p(k,c|\hat{\mathbf{Z}}_{1,N},\hat{\mathbf{F}}_{1,N})$ calculated for the set of simulated data used for Table 1. Figure 3 shows a comparison between the conditional PDFs $p(k|\hat{\mathbf{Z}}_{1,N},\hat{\mathbf{F}}_{1,N},\hat{c},\hat{\sigma}_{\eta f},\hat{\sigma}_{\eta z})$ and $p(c|\hat{\mathbf{Z}}_{1,N},\hat{\mathbf{F}}_{1,N},\hat{k},\hat{\sigma}_{\eta f},\hat{\sigma}_{\eta z})$, respectively, obtained from: (i) Eqs. (8) and (10) (crosses) and (ii) the Gaussian approximation $\mathcal{N}(\hat{\boldsymbol{\theta}},\mathbf{H}(\hat{\boldsymbol{\theta}})^{-1})$ described in Sec. 3.2 (solid). It is seen that the proposed Gaussian approximation is very accurate. Thus, the inverse Hessian matrix $\mathbf{H}(\hat{\boldsymbol{\theta}})^{-1}$ can be used to calculate the covariance matrix for the uncertainty in the value of the parameter $\boldsymbol{\theta}$, given the data $\hat{\mathbf{Z}}_{1,N}$ and $\hat{\mathbf{F}}_{1,N}$. In particular, this gives the variance $\sigma^2(\theta_j|\hat{\mathbf{Z}}_{1,N},\hat{\mathbf{F}}_{1,N})$ in Table 1 for each parameter θ_j of $\boldsymbol{\theta}$.

Another set of data is simulated with the same parameters except that the stiffness is reduced by 5%, i.e., $k=95$ N/m, to simulate damage. Identification results are shown in Table 2. By using the posterior PDFs for the undamaged and damaged oscillator, the probability of damage with respect to the fractional damage level d can be obtained. Figure 4 shows the probability of damage for different threshold levels d. It can be seen that it is almost with probability 1 that there is stiffness reduction in the damaged case. Furthermore, this damage is likely to be within the range from 0% to 10%, with median 5.6% and standard deviation 1.7%. The proposed approach is capable of indicating such a small level of damage with only a small amount of response data and unmeasured excitation that contributes about 63% of the rms response.

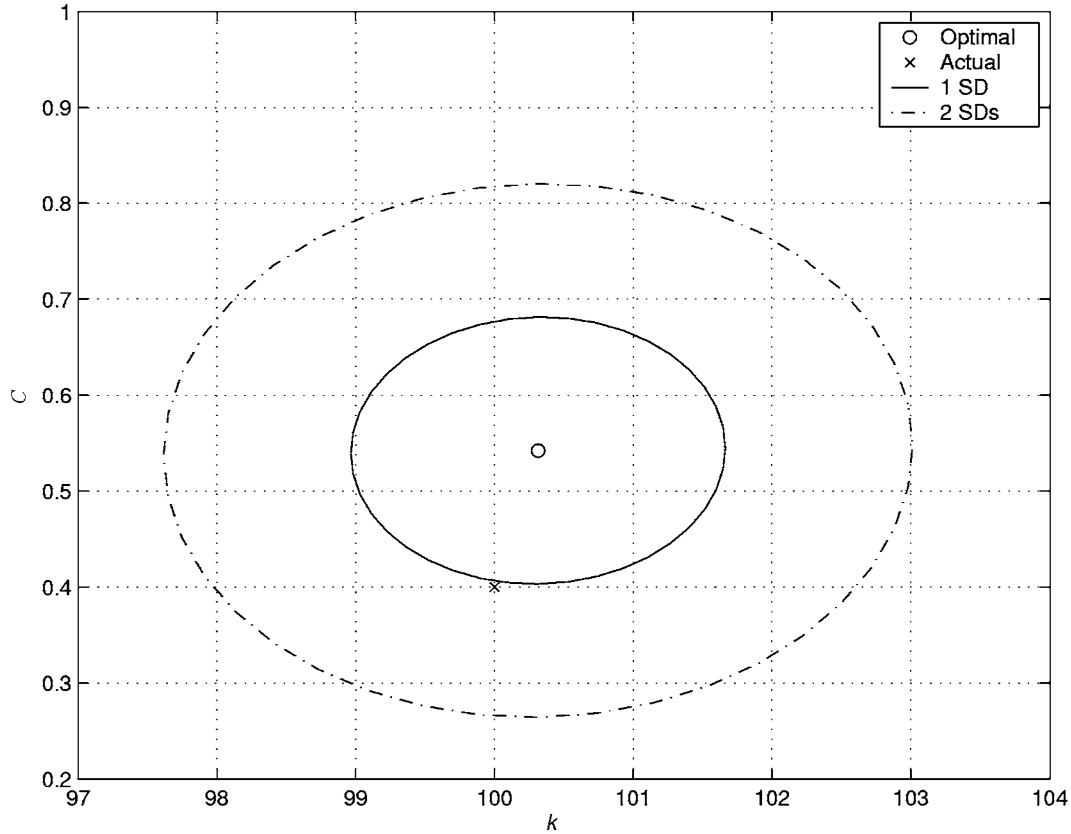

Fig. 2 Contours of the updated PDF projected onto the (k,c) plane of the undamaged oscillator (Example 1)

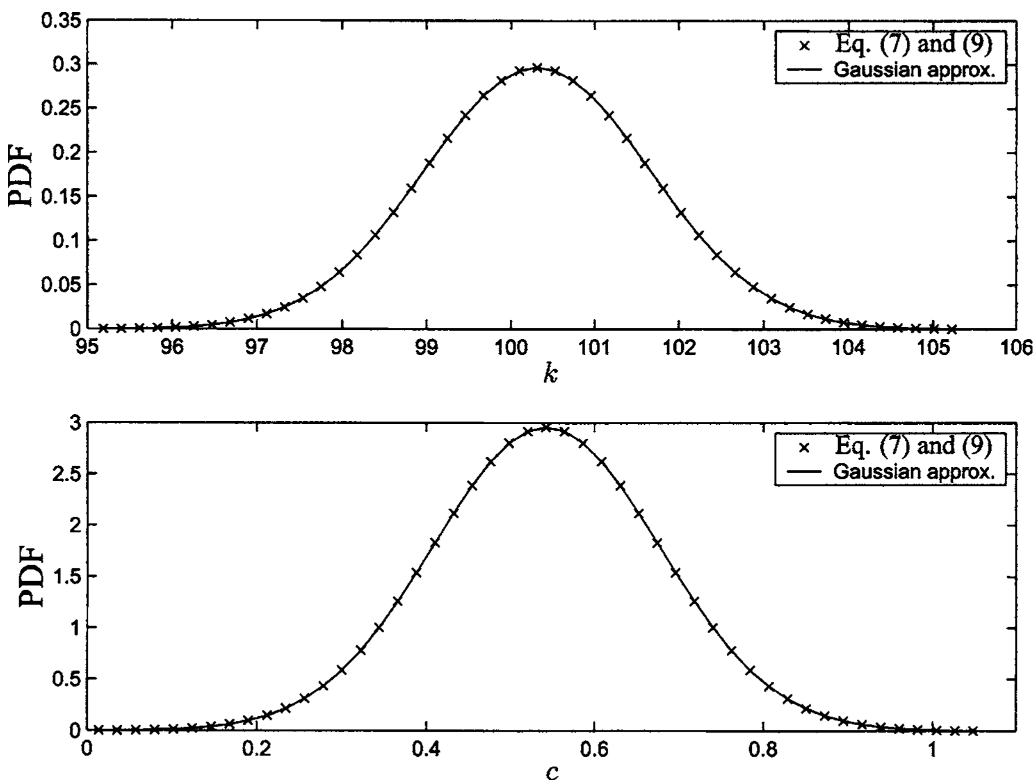

Fig. 3 Gaussian approximation for the conditional PDFs of the stiffness and damping coefficient of the undamaged oscillator (Example 1)

Table 2 Identification results of the stiffness parameters of the damaged oscillator (Example 1)

Parameter	Actual $\tilde{\theta}$	Optimal $\hat{\theta}$	S.D. σ	COV α	β
k	95.000	94.707	1.0805	0.011	0.27
c	0.4000	0.4099	0.1133	0.283	0.09
$\sigma_{\eta f}$	2.5005	2.5983	0.1059	0.042	0.93
$\sigma_{\eta z}$	0.0038	0.0039	0.0001	0.016	1.34

4.2 Example 2: Fifteen-Story Building Subjected to Earthquake and Wind Excitation. The second example uses simulated response data from the 15-story building shown in Fig. 5. The story height is 2.5 m. This building has uniformly distributed floor mass (100 ton each) and uniform story stiffness ($\tilde{k}_j=6.011 \times 10^5$ kN/m, $j=1,2,\ldots,15$), so that the first four modal frequencies are 1.250, 3.737, 6.186, and 8.571 Hz, respectively. Rayleigh damping is chosen so the damping matrix is given by $\mathbf{C}=\alpha_M\mathbf{M}+\alpha_K\mathbf{K}$, where $\tilde{\alpha}_M=0.1177$ s^{-1} and $\tilde{\alpha}_K=0.0006383$ s are used to simulate the data. As a result, the damping ratios of the first two modes are 1.0%.

For both undamaged and damaged cases, we assume that the measured response corresponds to the absolute acceleration at the 2nd, 5th, 8th, 11th and 14th DOF over a time interval $T=60$ s with a sampling interval $\Delta t=0.01$ s. Therefore, the total number of measured time points is $N=6000$ and corresponds to 48 fundamental periods.

The undamaged structure is subjected to stationary wind excitation (unmeasured) which has a uniform spectral intensity, $S_{f0}=5.0$ kN^2 s, at all DOFs and a correlation coefficient $\exp(-y/R)$, where y denotes the distance between two DOFs and R is a cor-

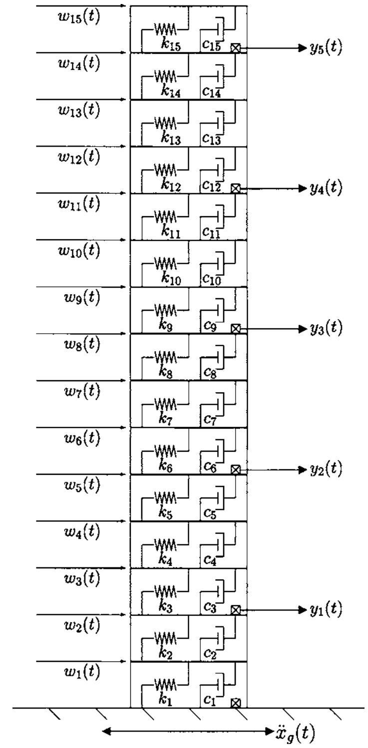

Fig. 5 Fifteen-story building model (Example 2)

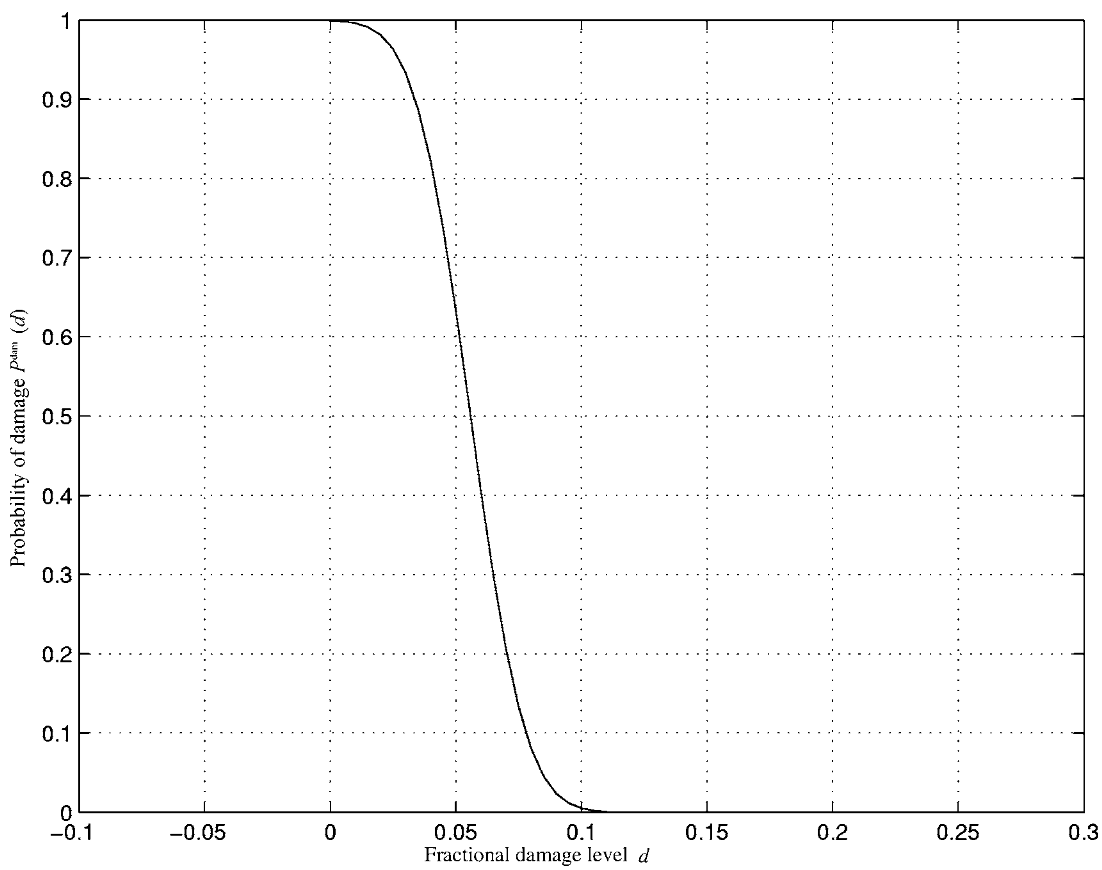

Fig. 4 Probability of damage for the stiffness (Example 1)

Table 3 Identification results of the undamaged structure (Example 2)

Parameter	Actual $\tilde{\theta}$	Optimal $\hat{\theta}$	S.D. σ	COV α	β
θ_1	1.0000	0.9978	0.0175	0.018	0.13
θ_2	1.0000	0.9909	0.0161	0.016	0.56
θ_3	1.0000	0.9939	0.0131	0.013	0.46
θ_4	1.0000	1.0071	0.0159	0.016	0.45
θ_5	1.0000	1.0224	0.0125	0.013	1.79
θ_6	1.0000	0.9849	0.0119	0.012	1.26
θ_7	1.0000	0.9848	0.0133	0.013	1.14
θ_8	1.0000	1.0228	0.0127	0.013	1.79
θ_9	1.0000	0.9779	0.0119	0.012	1.86
θ_{10}	1.0000	0.9987	0.0135	0.014	0.10
θ_{11}	1.0000	1.0076	0.0112	0.011	0.68
θ_{12}	1.0000	0.9812	0.0107	0.011	1.76
θ_{13}	1.0000	1.0083	0.0139	0.014	0.59
θ_{14}	1.0000	1.0187	0.0093	0.009	2.01
θ_{15}	1.0000	1.0047	0.0082	0.008	0.57
θ_{α_M}	1.0000	1.0062	0.4969	0.497	0.01
θ_{α_K}	1.0000	1.0165	0.0236	0.024	0.70
R	10.000	10.370	0.3753	0.038	0.99

relation distance, which is taken to be 10 m in the simulation of the data, but it is assumed unknown in the identification phase. The measurement noise for the response is taken to be 5%, i.e., the rms of the measurement noise for a particular channel of measurement is equal to 5% of the rms of the noise-free signal of the corresponding quantity. Identification using the proposed approach is carried out with a value of $N_p=100$, which corresponds to using previous data points of just over one fundamental period as the conditioning information at each time step in Eq. (10).

The stiffness and damping are based on the following nondimensional scaling parameters: stiffness parameters, $\theta_j, j=1,2,\ldots,15$ and damping parameters, θ_{α_M} and θ_{α_K}, that is, $k_j=\theta_j\tilde{k}_j$, $\alpha_M=\theta_{\alpha_M}\tilde{\alpha}_M$, and $\alpha_K=\theta_{\alpha_K}\tilde{\alpha}_K$. Table 3 shows the identification results for the undamaged structure. The second column in this table corresponds to the actual values of the parameters used for generation of the simulated measurement data; the third and fourth columns correspond to the most probable values and the calculated standard deviations, respectively; the fifth column lists the coefficient of variation for each parameter; and the last column shows the normalized error β described in Example 1. One observes that in all cases the actual parameters are at reasonable distances, measured in terms of the estimated standard deviations, from the most probable values, which confirms that the calculated uncertainties are consistent.

Figure 6 shows the contours in the (θ_1,θ_2) plane of the marginal updated PDF of θ_1 and θ_2. Figure 7 is a typical plot showing comparisons between the conditional PDFs of θ_1 and θ_2 (keeping all other parameters fixed at their most probable values) obtained from: (i) Eqs. (8) and (10) (crosses) and (ii) the Gaussian approximation $\mathcal{N}(\hat{\boldsymbol{\theta}},\mathbf{H}(\hat{\boldsymbol{\theta}})^{-1})$ described in Sec. 3.2 (solid). It is seen that the proposed Gaussian approximation is very accurate.

Next, damage is introduced by reducing the interstory stiffness of the first and third story by 15% and 10%, respectively. The damaged structure is subjected to wind excitation and earthquake ground motion. The wind excitation is assumed to have spectral intensity 2.5 kN^2 s with the same correlation model as before and the earthquake ground acceleration is taken to be equal to a 25% scaled version of the 1940 El-Centro earthquake N-S record.

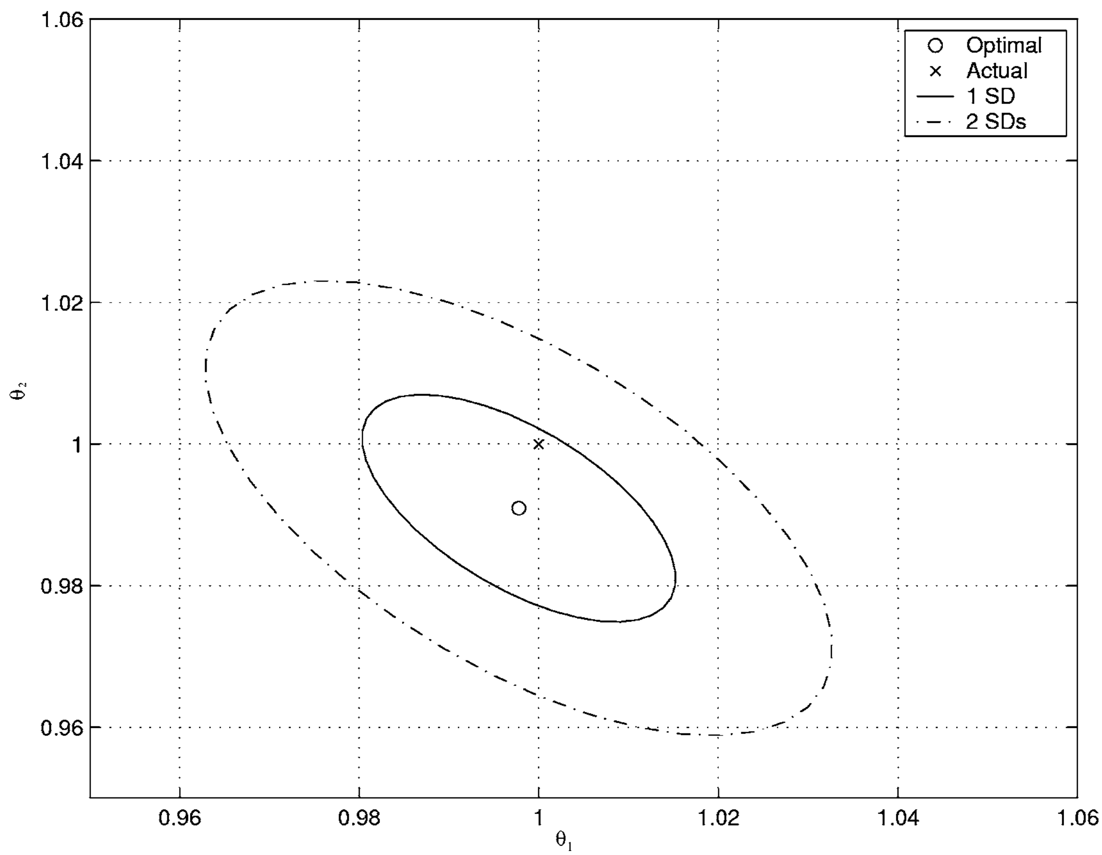

Fig. 6 Contours of the updated PDF projected onto the (θ_1,θ_2) plane of the undamaged structure (Example 2)

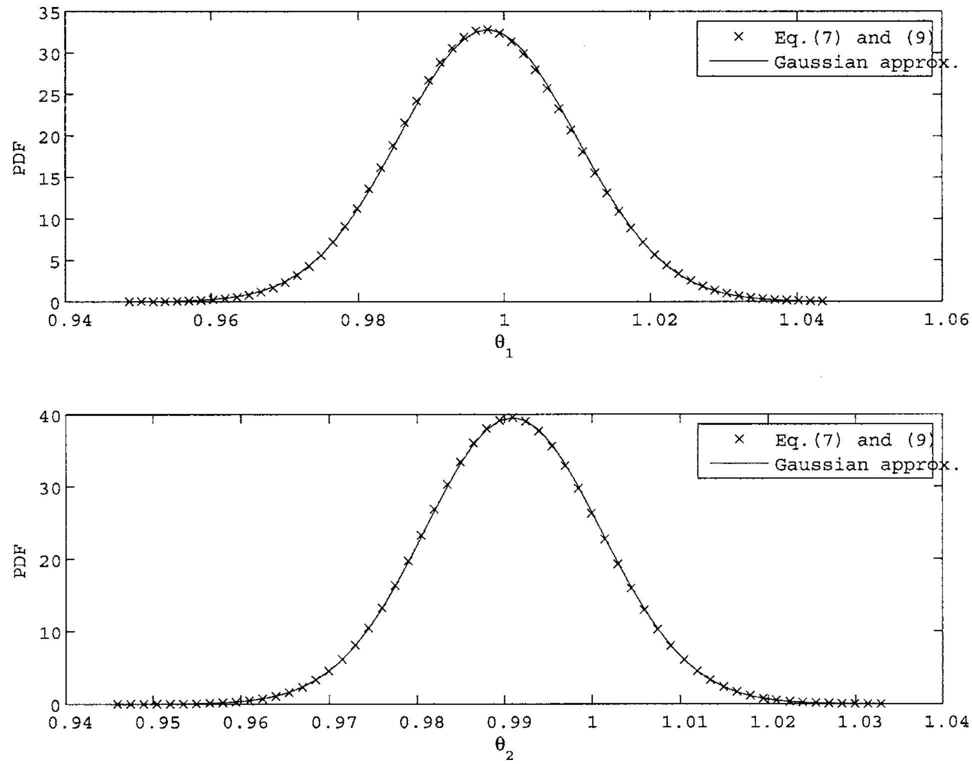

Fig. 7 Gaussian approximation for the conditional PDFs of the stiffness parameters θ_1 and θ_2 of the undamaged structure (Example 2)

Again, the wind excitation is assumed not to be measured but the earthquake ground motion is assumed to be measured with 5% measurement noise by a sensor at the base.

Figure 8 shows the displacement time histories at the first floor and the contribution from the earthquake only. Since the identification is based on acceleration, these data are assumed not to be available. It is shown here only for demonstration purposes. It can be seen that the earthquake ground motion dominates the response during the first 15 s but its contribution at later times is comparable with that from the wind excitation. If only the earthquake ground motion is considered, identification results will be poor, especially for the damping parameters, because the earthquake ground motion does not have much energy towards the end to explain the corresponding relatively strong response at these later times. Much smaller damping values, or even negative ones, will be identified in such case.

Identification results for the damaged structure are shown in Table 4. By using the posterior PDFs for the undamaged and damaged building, the probability of damage with respect to the fractional damage level can be obtained. Figure 9 shows the probability of damage with different threshold levels d. It can be seen that it is almost with probability 1 that there is stiffness reduction at the first and the third story. Furthermore, these damage levels have medians 14.8% and 10.5% and standard deviations 2.2% and 2.1%, respectively. The proposed approach is able to identify successfully both the location and severity of the damage. If a higher precision for the damage severity is desired, one solution is to obtain longer records of the structural excitation and response.

5 Concluding Remarks

A Bayesian approach to damage detection, location and assessment is presented using noisy incomplete excitation and response data. It is based on an approximate conditional probability density expansion of the updated PDF of the model parameters of a linear MDOF system using dynamic data. The updated posterior PDF can be accurately approximated by a multi-variate Gaussian distribution where the calculated mean and covariance matrix offer an estimate of the most probable values of the model parameters and their associated uncertainties. The updated PDFs from data in the undamaged state and in a possibly damaged state are used to calculate the probability of damage of different severity levels in each substructure. The approach was shown to successfully determine the location and probable level of damage from noisy incomplete data.

Acknowledgment

The first author would like to gratefully acknowledge the generous support by the Research Committee of University of Macau under Grant Nos. RG030/02-03S/YKV/FST and RG097/03-04S/YKV/FST.

Appendix A

Using Eqs. (4) and (13)–(15), the prediction error $\boldsymbol{v}[k]$ can be expressed as follows

$$\begin{aligned}\boldsymbol{v}[k] &= \mathbf{z}[k] - \boldsymbol{\mu}[k] \\ &= \mathbf{L}_1\mathcal{L}(k;\boldsymbol{\theta}^{\star},[\boldsymbol{\eta}_f[1],\ldots,\boldsymbol{\eta}_f[k-1]]) + \mathbf{L}_2\boldsymbol{\eta}_f[k] + \boldsymbol{\eta}_z[k] \\ &= \mathbf{L}_1\sum_{m=1}^{k-1}\mathbf{A}_d^{m-1}\mathbf{B}_d\boldsymbol{\eta}_f[k-m] + \mathbf{L}_2\boldsymbol{\eta}_f[k] + \boldsymbol{\eta}_z[k]\end{aligned} \tag{28}$$

where the parameter vector $\boldsymbol{\theta}^*$ has zero initial conditions and all other parameters are equal to the corresponding parameters in $\boldsymbol{\theta}$.

The covariance matrix $\Sigma_v[k,k+r] \equiv E[\boldsymbol{v}[k]\boldsymbol{v}^T[k+r]]$, $r \geqslant 0$, is given by

$$\begin{aligned}\Sigma_v[k,k+r] = \mathbf{L}_1\left[\sum_{m=1}^{k-1}\mathbf{A}_d^{m-1}\mathbf{B}_d\Sigma_{\eta f}\mathbf{B}_d^T(\mathbf{A}_d^T)^{m-1}\right](\mathbf{A}_d^T)^r\mathbf{L}_1^T \\ + \mathbf{L}_2\Sigma_{\eta f}\mathbf{B}_d^T(\mathbf{A}_d^T)^{r-1}\mathbf{L}_1^T(1-\delta_{r,0}) + (\mathbf{L}_2\Sigma_{\eta f}\mathbf{L}_2^T + \Sigma_{\eta z})\delta_{r,0}\end{aligned} \tag{29}$$

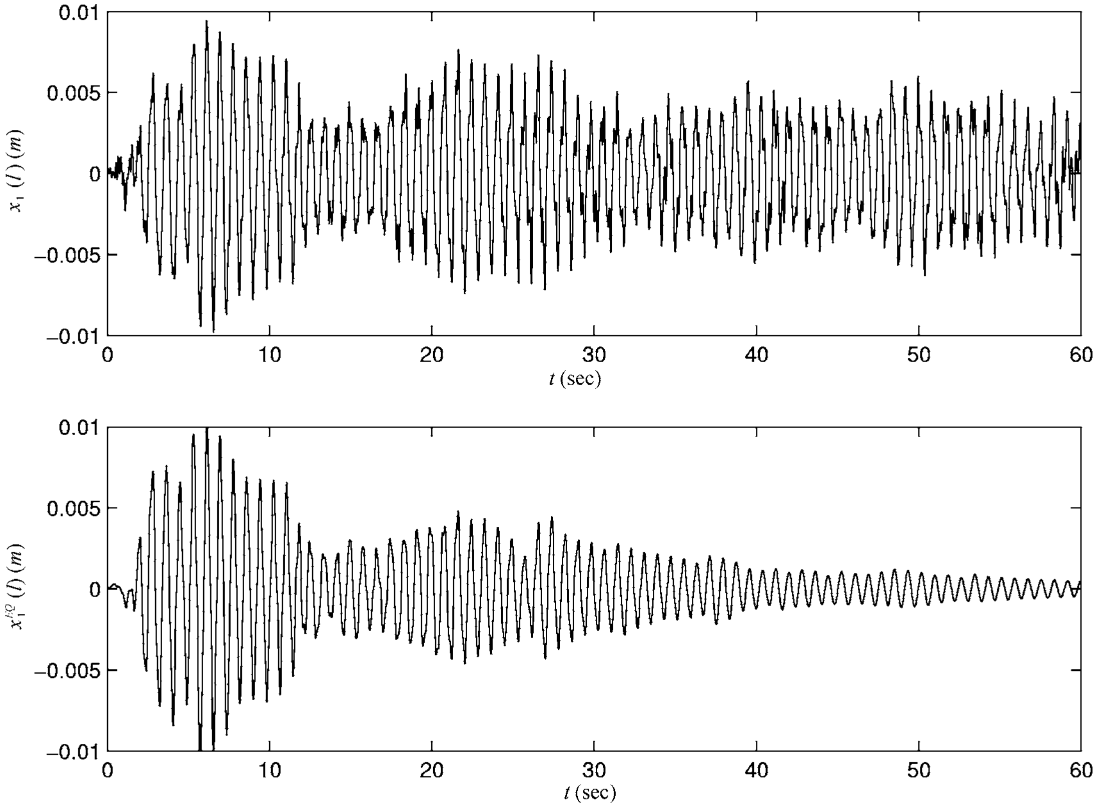

Fig. 8 Response time history (top) and its contribution from the earthquake only (bottom) at the first floor of the damaged structure (Example 2)

The sum $\mathbf{S}_k=\Sigma_{m=1}^{k-1}\mathbf{A}_d^{m-1}\mathbf{B}_d\Sigma_{\eta f}\mathbf{B}_d^T(\mathbf{A}_d^T)^{m-1}$ can be calculated by solving the following Lyapunov equation in discrete form [29]

$$\mathbf{S}_k=\mathbf{A}_d\mathbf{S}_k\mathbf{A}_d^T+[\mathbf{B}_d\Sigma_{\eta f}\mathbf{B}_d^T-\mathbf{A}_d^{k-1}\mathbf{B}_d\Sigma_{\eta f}\mathbf{B}_d^T(\mathbf{A}_d^T)^{k-1}] \quad (30)$$

For dissipative dynamical systems, the two-norm of the matrix $\mathbf{A}_d$ is less than unity, i.e., $\|\mathbf{A}_d\|_2<1$. As a result, the term $\mathbf{A}_d^{k-1}\mathbf{B}_d\Sigma_{\eta f}\mathbf{B}_d^T(\mathbf{A}_d^T)^{k-1}\to 0$ for large k. Therefore, Eq. (30) can be approximated by

$$\mathbf{S}_\infty=\mathbf{A}_d\mathbf{S}_\infty\mathbf{A}_d^T+\mathbf{B}_d\Sigma_{\eta f}\mathbf{B}_d^T \quad (31)$$

The advantage of this approximation is that the matrix $\mathbf{S}_\infty$ is no longer dependent on k, which improves the computational efficiency significantly.

Thus, the covariance matrix $\Sigma_v[k,k+r]$, $r\geqslant 0$, is readily obtained:

$$\Sigma_v[k,k+r]=\mathbf{L}_1\mathbf{S}_\infty(\mathbf{A}_d^T)^r\mathbf{L}_1^T+\mathbf{L}_2\Sigma_{\eta f}\mathbf{B}_d^T(\mathbf{A}_d^T)^{r-1}\mathbf{L}_1^T(1-\delta_{r,0}) + (\mathbf{L}_2\Sigma_{\eta f}\mathbf{L}_2^T+\Sigma_{\eta z})\delta_{r,0} \quad (32)$$

Note that the right hand side of this expression does not depend on k.

Table 4 Identification results of the damaged structure (Example 2)

Parameter	Actual $\tilde{\theta}$	Optimal $\hat{\theta}$	S.D. σ	COV α	β
θ_1	0.8500	0.8495	0.0125	0.015	0.04
θ_2	1.0000	1.0103	0.0136	0.014	0.76
θ_3	0.9000	0.8887	0.0110	0.012	1.03
θ_4	1.0000	0.9938	0.0142	0.014	0.44
θ_5	1.0000	1.0074	0.0126	0.013	0.59
θ_6	1.0000	0.9758	0.0117	0.012	2.06
θ_7	1.0000	1.0214	0.0149	0.015	1.43
θ_8	1.0000	0.9979	0.0124	0.012	0.17
θ_9	1.0000	0.9759	0.0116	0.012	2.07
θ_{10}	1.0000	1.0293	0.0145	0.015	2.02
θ_{11}	1.0000	0.9971	0.0115	0.012	0.26
θ_{12}	1.0000	0.9981	0.0108	0.011	0.18
θ_{13}	1.0000	1.0129	0.0140	0.014	0.92
θ_{14}	1.0000	1.0062	0.0098	0.010	0.63
θ_{15}	1.0000	1.0024	0.0081	0.008	0.29
θ_{α_M}	1.0000	1.0149	0.2823	0.282	0.05
θ_{α_K}	1.0000	1.0248	0.0234	0.023	1.06
R	10.000	10.007	0.3649	0.037	0.02

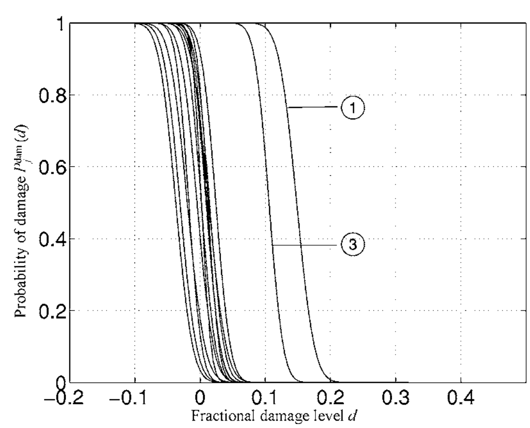

Fig. 9 Probability of damage for the stiffness parameters θ_j, $j=1,\ldots,15$ (Example 2)

References

[1] Natke, H. G., and Yao, J. T. P., eds., 1988, *Proceedings of the Workshop on Structural Safety Evaluation Based on System Identification Approaches*, Vieweg, Wiesbaden.

[2] Agbabian, M. S., and Masri, S. F., eds., 1988, *Proceedings of the International Workshop on Nondestructive Evaluation for Performance of Civil Structures*. Los Angeles, CA: Department of Civil Engineering, University of Southern California.

[3] Chang, F. K., ed., 2003, *Proceedings of the 4th International Workshop on Structural Health Monitoring*, Stanford University.

[4] Mazurek, D. F., and DeWolf, J. T., 1990, "Experimental Study of Bridge Monitoring Technique," J. Struct. Eng., **116**(9), pp. 2532–2549.

[5] Hearn, G., and Testa, R. B., 1991, "Modal Analysis for Damage Detection in Structures," J. Struct. Eng., **117**(10), pp. 3042–3063.

[6] Doebling, S. W., Farrar, C. R., Prime, M. B., and Shevitz, D. W., 1996, "Damage Identification and Health Monitoring of Structural and Mechanical Systems From Changes in Their Vibrations Characteristics: A Literature Review," Technical Report, LA-13070-MS, Los Alamos National Laboratory.

[7] Lam, H. F., Ko, J. M., and Wong, C. W., 1998, "Localization of Damaged Structural Connections Based on Experimental Modal and Sensitivity Analysis," J. Sound Vib., **210**(1), pp. 91–115.

[8] Smyth, A. W., Masri, S. F., Caughey, T. K., and Hunter, N. F., 2000, "Surveillance of Intricate Mechanical Systems on the Basis of Vibration Signature Analysis," J. Appl. Mech., **67**(3), pp. 540–551.

[9] Farhat, C., and Hemez, F. M., 1993, "Updating Finite Element Dynamics Models Using Element-by-Element Sensitivity Methodology," AIAA J., **31**(9), pp. 1702–1711.

[10] Pandey, A. K., and Biswas, M., 1994, "Damage Detection in Structures Using Changes in Flexibility," J. Sound Vib., **169**, pp. 3–17.

[11] Kim, H. M., Bartkowicz, T. J., Smith, S. W., and Zimmerman, D., 1995, "Health Monitoring of Large Structures," J. Sound Vib., **29**(4), pp. 18–21.

[12] Topole, K. G., and Stubbs, N., 1995, "Non-Destructive Damage Evaluation in Complex Structures From a Minimum of Modal Parameters," Int. J. Anal. Exp. Modal Anal., **10**(2), pp. 95–103.

[13] Hemez, F. M., and Farhat, C., 1995, "Structural Damage Detection via a Finite Element Model Updating Methodology," Int. J. Anal. Exp. Modal Anal., **10**(3), pp. 152–166.

[14] Katafygiotis, L., S., Papadimitriou, C., and Lam, H. F., 1998, "A Probabilistic Approach to Structural Model Updating," Soil Dyn. Earthquake Eng., **17**(7–8), pp. 495–507.

[15] Doebling, S. W., Farrar, C. R., and Prime, M. B., 1998, "A Review of Damage Identification Methods That Examine Changes in Dynamics Properties," Shock Vib. Dig., **30**(2), pp. 91–105.

[16] Vanik, M. W., Beck, J. L., and Au, S. K., 2000, "Bayesian Probabilistic Approach to Structural Health Monitoring," J. Eng. Mech., **126**(7), pp. 738–745.

[17] Beck, J. L., Au, S. K., and Vanik, M. W., 2001, "Monitoring Structural Health Using a Probabilistic Measure," Comput. Aided Civ. Infrastruct. Eng., **16**, pp. 1–11.

[18] Sohn, H., and Farrar, C. R., 2001, "Damage Diagnosis Using Time Series Analysis of Vibration Signals," Smart Mater. Struct., **10**, pp. 1–6.

[19] Ko, J. M., Sun, Z. G., and Ni, Y. Q., 2002, "Multi-Stage Identification Scheme for Detecting Damage in Cable-Stayed Kap Shui Mun Bridge," Eng. Struct., **24**(7), pp. 857–868.

[20] Ching, J., and Beck, J. L., 2004, "New Bayesian Model Updating Algorithm Applied to a Structural Health Monitoring Benchmark," Struct. Health Monit., **3**, pp. 313–332.

[21] Geyskens, P., Der Kiureghian, A., and Monteiro, P., 1998, "Bayesian Prediction of Elastic Modulus of Concrete," J. Struct. Eng., **124**(1), pp. 89–95.

[22] Beck, J. L., and Katafygiotis, L. S., 1998, "Updating Models and Their Uncertainties. I: Bayesian Statistical Framework," J. Eng. Mech., **124**(4), pp. 455–461.

[23] Katafygiotis, L. S., and Yuen, K.-V., 2001, "Bayesian Spectral Density Approach for Modal Updating Using Ambient Data," Earthquake Eng. Struct. Dyn., **30**(8), pp. 1103–1123.

[24] Yuen, K.-V., 2002, "Ph.D. Thesis: Model Selection, Identification and Robust Control for Dynamical Systems," Technical Report No. EERL 2002–03, California Institute of Technology, Pasadena.

[25] Yuen, K.-V., and Katafygiotis, L. S., 2002, "Bayesian Modal Updating Using Complete Input and Incomplete Response Noisy Measurements," J. Eng. Mech., **128**(3), pp. 340–350.

[26] Yuen, K.-V., Au, S. K., and Beck, J. L., 2004, "Two-Stage Structural Health Monitoring Methodology and Results for Phase I Benchmark Studies," J. Eng. Mech., **130**(1), pp. 16–33.

[27] Jaynes, E. T., 2003, *Probability Theory: The Logic of Science*, L. Bretthorst (ed.), Cambridge University Press.

[28] MATLAB, 1994, *Matlab User's Guide*, The MathWorks, Inc., Natick, MA.

[29] Lin, Y. K., 1976, *Probabilistic Theory of Structural Dynamics*, Krieger, Malabar, FL.